Cooperation between Cancer Cells and Regulatory T Cells to Promote Immune-escape through Integrin αvβ8-Mediated TGF-β Activation

Alexandra Laine
Cancer Research Center of Lyon
Ossama Labiad
Cancer Research Center of Lyon
Hector Hernandez-Vargas
French Institute of Health and Medical Research https://orcid.org/0000-0001-6045-2103
Sebastien This
University of Oxford
Amélien Sanlaville
Cancer Research Center of Lyon https://orcid.org/0000-0002-0865-8005
Sophie Leon
Centre Léon Bérard
Stéphane Dalle
Centre de Recherche en Cancérologie de Lyon, Hospices Civils de Lyon
Dean Sheppard
University of California, San Francisco https://orcid.org/0000-0002-6277-2036
Mark Travis
Manchester University
Helena Paidassi
International Center for Infectiology Research, University of Lyon, Lyon, France https://orcid.org/0000-0001-9915-4365
Julien Marie (julien.marie@inserm.fr)
Cancer Research Center of Lyon https://orcid.org/0000-0001-6713-7923

Article

Keywords: cancer cells, immunosuppression, T cells (Tregs), TGF-b

Posted Date: February 18th, 2021

DOI: https://doi.org/10.21203/rs.3.rs-208701/v1

Version of Record: A version of this preprint was published at Nature Communications on October 28th, 2021. See the published version at https://doi.org/10.1038/s41467-021-26352-2.

Abstract

Among the strategies allowing cancer cells to escape the immune system, the presence of TGF-b in the tumor micro-environment is one of the most potent. However, TGF-b is secreted in an inactive form and mechanisms responsible for its activation within the tumor remain unknown. Here, we demonstrate that regulatory T cells (Tregs) compose the main cells expressing the b8 chain of avb8 integrin (Itgb8) in the tumors and that the Itgb8^{pos} Treg population activates TGF-b produced by the cancer cells and stored in the tumor micro-environment. Itgb8 ablation in Tregs impaired TGF-b signaling in T lymphocytes present in the tumor but not in the tumor draining lymph nodes. The cytotoxic function of CD8^{pos} T lymphocytes infiltrating the tumors was subsequently exacerbated leading to an efficient control of the tumor growth. Similar observations were made in patient tumors after anti-Itgb8 antibody treatment. Thus, this study reveals that Tregs work in concert with cancer cells to produce bioactive-TGF-b and create a powerful-immunosuppressive micro-environment.

Introduction

The tenet of tumor immunotherapy is based on the ability of the immune system to survey for malignant transformation and be efficient at eliminating cancer cells. However, solid tumors can escape from the immune system by orchestrating a micro-environment that limits an efficient anti-tumor immune response.

In the tumor micro-environment, Transforming Growth Factor beta (TGF-β) is regarded as a key cytokine promoting potent immunosuppression [1]. Among the three isoforms of TGF-β (TGF-β 1–3), TGF-β1 is prevalent within tumors [2 3]. This polypeptide cytokine, highly conserved in all mammals [4], impairs numerous functions of effector T lymphocytes and promotes both development and stability of CD4^{pos} Foxp3^{pos} regulatory T cells (Tregs) [5, 6]. Subsequently, the selective targeting of TGF-β signaling in T lymphocytes leads to an efficient elimination of cancer cells by effector T lymphocytes [7] repressing their cytotoxic functions [8]. Hence, neutralization of TGF-β-immunoregulatory effects has been thought of as a promising anti-cancer therapy. However, major safety issue were raised, one of which being the risk of unleashing massive autoimmunity, given the key role of TGF-b signaling in the repression of T lymphocytes activation [5, 6 9 10].

Importantly, TGF-β is one of the few cytokines secreted in an inactive form. This small latency complex is composed of the mature cytokine encircled by the latency-associated peptide (LAP), which are non-covalently associated. LAP covers all the contact sites of the mature cytokine that must interact with TGF-β receptor complexes (TGFβRI and TGFβRII) to induce TGF-β signaling, including the phosphorylation of SMAD2/3 [11]. Within solid tumors, the latent TGF-β complex can be secreted by several cell types, including cancer cells, and Tregs [1]. Nevertheless, unlike the TGF-β produced by Tregs, TGF-β secreted by cancer cells seems essential for the repression of the anti-tumor immune response [12, 13]. As long as LAP maintains close contacts with the mature cytokine, the secreted latent TGF-β can be

stored in the tumor micro-environment, attached to the extracellular matrix, without any immune regulatory functionality [14]. Hence, activation of the secreted TGF-β latent complex, which involves exposure of the receptor-binding domain of the mature cytokine, is therefore indispensable for TGF-β-mediated immune regulatory functions in tumors. Thus, deciphering the mechanisms by which the activation of TGF-β present in the tumor micro-environment occurs is essential to our comprehension of solid tumors escape the immune system and will highlight potential new effective anti-cancer therapies that specifically target TGF-β activation within the tumor micro-environment and thus limiting autoimmune side effects associated to the privation of TGF-b activation

In this study, we demonstrate that the expression of the integrin αvβ8 in Tregs is essential to efficiently activate TGF-β produced by cancer cells and promote tumor immune escape. In the absence of expression of the β8 integrin chain (Itgβ8) in Tregs, TGF-β signaling is impaired in tumor infiltrating effector T cells and their cytotoxic functions are unleashed leading to the efficient control of tumor growth. In patient tumors, treatment with a neutralizing anti-Itgβ8 antibody, as well as single-cell gene expression analysis on tumor infiltrating T cells, confirmed the relevance of our findings in mice to human pathology. Overall, our results reveal an unexpected collaboration between cancer cells and Tregs to create an efficient TGF-β-mediated immunosuppressive tumor micro-environment (TME), highlighting that the targeting of Itgβ8 could constitute an efficient novel immunotherapies.

Results

Itgβ8 is mainly expressed in regulatory T cells in tumors

In vivo, the activation of TGF-β1 is largely dependent on integrins, including the αvβ8 integrin, whose expression is regulated by that of the β8 subunit (Itgβ8) [11 15]. In order to understand the mechanisms leading to the activation of the latent complex in the tumor, we first analyzed Itgβ8 cellular expression in the TME.

To monitore Itgβ8 by flow cytometry, we took an unbiased approach by generating an *Itgb8-td-Tomato* reporter mice, in which we previously validated that td-tomato positive cells expressed Itgb8 protein in different cell types, including T lymphocytes [16]. Flow cytometry analysis of tumors (melanoma and breast cancer) revealed that among host cells composing the TME, Itgβ8^{pos} cells were mainly (85–95%) CD45^{pos} hematopoietic cells (Fig. 1A-B). T lymphocytes (CD3^{pos}), and particularly the CD4^{pos} Foxp3^{pos} (Treg) subset, composed the main portion of hematopoietic cells expressing Itgβ8, with approximately 80% of Itgβ8^{pos} CD45^{pos} cells being CD4^{pos} Foxp3^{pos} irrelevant of the tumor type (Fig. 1C-F). Moreover, within the Treg compartment, we found that about 40–45% of cells expressed Itgβ8 (Fig. 1G-H) and only Itgβ8^{pos} Tregs were endowed with the capacity to efficiently activate TGF-β1 (Figure 1I) whereas both Itgβ8^{pos} Treg and Itgβ8^{neg}Treg populations expressed similar levels of this cytokine (Figure 1J). Thus, this first set of data reveals that Tregs constitute a large part of the Itgβ8-expressing host cells within the TME.

Itgβ8 expression in Tregs impairs anti-tumor response and promotes tumor-growth

Next, in order to assess whether Itgβ8 expression by Tregs confers them abilities to control the anti-tumor immune responses by providing a bioactive source of TGF-b, we first selectively ablated *Itgb8* in Tregs, using *Foxp3-Cre Itgb8$^{fl/fl}$* mice (Foxp3$^{\Delta Itg\beta 8}$). Importantly, in Foxp3$^{\Delta Itg\beta 8}$ mice Tregs retain their numbers, localization, as well as their suppressive functions, including the ability to produce TGF-β1. Moreover, no autoimmunity signs, neither uncontrolled effector T cell activation have been observed in Foxp3$^{\Delta Itg\beta 8}$ animals [17, 18].

Strikingly, in contrast to their littermate controls (Foxp3^{Ctrl}), Foxp3$^{\Delta Itg\beta 8}$ mice showed a profound impairment of tumor growth irrelevant of the tumor type **(**Fig. 2A-F**)**. Notably, we observed that 25–50% of the Foxp3$^{\Delta Itg\beta 8}$ animals exhibited a complete control of the tumor progression depending of the tumor type (**Figure G-H)**. Thus, Itgβ8 expression in Tregs promoted tumor growth, implying that the Itgβ8^{pos} Treg population could affect the anti-tumor function of the effector T cells.

To confirm this scenario, we next analyzed the immune compartment of tumors and that of their draining lymph nodes (tdLN). Interestingly, the proportion of Natural Killers (NK) cells and T cells, including Tregs, were similar in both TME and tdLN between Foxp3$^{\Delta Itg\beta 8}$ mice and Foxp3^{Ctrl} animals **(Figure S1A)**. In line with this observation, the proliferative status of T cells and NK cells was similar between Foxp3$^{\Delta Itg\beta 8}$ mice control animals in both tdLN and TME **(Figure S1B)**. Moreover, the deprivation of Itgb8 on Tregs failed to affect the distribution of T lymphocytes within the TME (data not shown). Thus, we ruled-out a specific role of the Itgβ8^{pos} Tregs in controlling proliferation, recruiting of effector immune T cells into the TME as well as T cell priming in tdLN. However, the inhibition of tumor-growth observed in Foxp3$^{\Delta Itg\beta 8}$ mice was completely lost when animals were depleted of their CD8^{pos} T lymphocytes **(**Fig. 3A-B**)**.

Thus, altogether these observations suggested that Itgβ8^{pos} Tregs exert their pro-tumoral effects by impairing the anti-tumor functions of CD8^{pos} T lymphocytes. In agreement with this assumption, we observed that CD8^{pos} T lymphocytes of the TME of Foxp3$^{\Delta Itg\beta 8}$ mice exhibited higher cytotoxic functions based on the production of granzyme B cytotoxic granules (GzB) in association with the surface expression of CD107 (Lamp1) compared to Foxp3^{Ctrl} animals **(**Fig. 3C**)**. Production of IFN-γ was also exacerbated in tumor infiltrating in both CD4^{Pos} T cells and CD8^{pos} T cells from Foxp3$^{\Delta Itg\beta 8}$ mice compared to Foxp3^{Ctrl} animals (**Figure S2**).

Supporting the exacerbated cytotoxic features of CD8^{pos} T lymphocytes in the TME of Foxp3$^{\Delta Itg\beta 8}$ mice, as well as the control of tumor growth in these animals, histology analysis showed higher numbers of apoptotic cells in tumors from Foxp3$^{\Delta Itg\beta 8}$ mice than control animals **(**Fig. 3D-E**)**. Importantly, in clear contrast to the TME, we failed to find any exacerbation of the cytotoxic phenotype of CD8^{pos} T cells in the tdLN of Foxp3$^{\Delta Itg\beta 8}$ mice **(**Fig. 3F**)**. This observation, combined with the absence of systemic T effector cell activation in secondary lymphoid organs of in Foxp3$^{\Delta Itg\beta 8}$ mice [17, 18], reveals a specific role for

Itgβ8^{pos} Tregs in the repression of the cytotoxic functions of CD8^{pos} T lymphocytes selectively in the TME.

Altogether, these data identify Itgβ8 as a key mediator of Treg induced suppression of the anti-tumor cytotoxic function of CD8^{pos} T cells present in the TME with direct consequences on tumor progression.

Itgβ8 expression on Tregs promotes TGF-β signaling controlling effector tumor T cells

Given the role of αvβ8 in TGF-β activation [11], and the unique ability of the Itgβ8^{pos} Treg subset to activate TGF-β1 compared to Itgβ8^{neg} Tregs (**figure 1I**), we next assessed whether the repression of CD8^{pos} T cell cytotoxic functions in the TME of Foxp3$^{\Delta Itg\beta 8}$ mice was due to an increase of the TGF-β signaling in the effector cells in the tumor. This assumption was even more motivated by the fact that, we found that the percentage of T cells with high activation of TGF-β signaling pathway, monitored by the phosphorylation of SMAD2-3, was halved in the TME of Foxp3$^{\Delta Itg\beta 8}$ mice compared to Foxp3^{Ctrl} animals (Fig. 4A). Notably, in contrast to the TME, and in line with the absence of T cell over activation in tdLN of Foxp3$^{\Delta Itg\beta 8}$ mice the levels of phosphorylation of SMAD2-3 in T lymphocytes from tdLN were similar between Foxp3$^{\Delta Itg\beta 8}$ mice and Foxp3^{Ctrl} animals (Fig. 4B). Hence, Itgβ8^{pos} Tregs are responsible of the increase of TGF-b signaling in T cells present in the TME.

In order to confirm that the exacerbated cytotoxic features of CD8^{pos} T cells in the TME of Foxp3$^{\Delta Itg\beta 8}$ mice were directly linked to the increase TGF-β signaling in effector T cells by Itgβ8^{pos} Tregs, we developed genetic approaches allowing to sustain high levels of TGF-β signaling activation in effector T cells. The T cell compartment of CD3ε deficient mice was reconstituted with purified Tregs from either Foxp3^{Ctrl} mice or Foxp3$^{\Delta Itg\beta 8}$ mice and Foxp3^{neg} T cells expressing either a constitutively active (CA) form (TGFβRI^{CA}) or the unmodified form of TGFβRI (TGFβRI^{WT}) [19] (Fig. 4C). In TGFβRI^{CA}-expressing T cells, the TGF-β signaling pathway remains activated even in the absence of bio-active source of TGF-β in their micro-environment as we previously described it [19, 20]. Similarly to data illustrated in Fig. 3C, we observed that the absence of Itgβ8 expression in Tregs (Treg$^{\Delta Itg\beta 8}$) increased the cytotoxic features of transferred wild type CD8^{pos} T cells. In contrast, the maintenance of TGF−β signaling in effector T cells was sufficient to completely prevent the over-activation of their cytotoxic program as well as the repression of tumor growth we routinely observed in the absence of Itgβ8 expression on Tregs (Fig. 4D-E). Thus, within the TME, Itgβ8 expression on Tregs increases the levels of TGF-β signaling activation in effector T lymphocytes which is sufficient to repress their cytotoxic functions.

Activation of cancer-cell-produced TGF-β1 by Itgβ8^{pos}Tregs leads to tumor CD8 T cell loss of function

Our aforementioned data, combined with inability of Itgb8 expression to modulate *Tgf-b1* expression in Tregs (Fig. 1I) and the minor role of TGF-β1-produced by Tregs in the control of the effector T cell functions in the TME [12], strongly suggest that Itgb8^{pos} Tregs could contribute to the activation of TGF-b1 produced by other cells of the TME. As LAP reflects the inactive form of TGF-β, we evaluated the presence

of LAP within the TME either in the presence or in the absence of Itgβ8 in Tregs. Strikingly, the classic fibrillar staining of the large latent complex was 2–3 times increased in the TME of Foxp3$^{\Delta Itg\beta 8}$ mice compared to Foxp3^{Ctrl} animals (Fig. 5A-B). In order to address, the source of inactive TGF-b1 which accumulate in the TME of Foxp3$^{\Delta Itg\beta 8}$ mice, we selective ablated *tgf-b1* in cancer cells regarded as high producer cells of TGF-b1 (TGF-β1^{KO}) in the TME [23] (**Figure S3A).** The accumulation of inactive form of TGF-β1 was lost in the TME of TGF-β1^{KO} cancer cells (Fig. 5C**)**. Of note, the absence of TGF-b1 production by cancer cells strongly impaired the tumor growth in wild-type mice but not in T cell deficient animals (CD3^{KO}) (**Figure S3B C)**. Confirming the importance of TGF-b1 produced by cancer cells in the control of T cell anti-tumor immune response, the cytotoxic functions of CD8 T cells from the TME of TGF-β1^{KO} cancer cells were 2–3 times exacerbated TGF-β1 sufficient cancer cells (Fig. 5D-E**)**. Importantly the production of TGF-b1 by cancer cells had no significant impact Treg homeostasis **(Figure S3D)** and T cell activation in the tdLN **(Figure S3E-F).** Thus, Itgb8 expression by Tregs contributes to the activation TGF-b1 produced by cancer cells in the TME, with direct consequences on the repression the cytotoxic functions of CD8^{pos} T cells present in the TME and thus on tumor immune escape .

Itgβ8 expression on tumor infiltrating T cells is associated with poor patient survival and CD8 T cell activation

We next analyzed the relevance of our data in mice to the human pathology particularly in melanoma patients. First, we confirmed that human T cells expressed *ITGb8* in the TME by analyzing single-cell mRNAseq, and reported that *ITGB8* expression was prevalent in the Foxp3^{pos} compartment of the TME of various tumor types, with 65–70% of Itgβ8^{pos} T cells being Foxp3^{pos} T cells (**Figure S4**). We then made use of publicly available sets of single cell-sequencing analysis data and obtained a specific gene-expression signature of Itgβ8^{pos} T cells infiltrating the tumors, allowing us to perform multivariable survival analysis. We analyzed 358 patients bearing melanoma and revealed that high *ITGB8* score in tumor infiltrating T cells was associated with poor survival (Fig. 6A**).** Of note the poor survival prognostic associated to presence of Itb8 Tregs was confirmed in other tumor types except in colorectal cancer (**Figure S5**) The better survival prognostic observed in colorectal patients with high *ITGB8* score in Tregs from the TME was in agreement with the ability of Itgβ8^{pos} Tregs to repress established chronic intestinal inflammation in mice [18] which was largely depicted to promote colorectal cancer progression [21]. Interestingly, our analysis confirmed that *FOXP3* expression alone in the T cells of TME was not sufficient to predict patient prognosis in any tumor types as previously showed [22] (**Figure S5**). Of note, given that *ITGB8* expression was reported to be increased on activated human Tregs [18], we also removed the gene signature of activated Tregs in the *ITGB8* Treg signature and obtained similar survival prognostics as with the *ITGB8* Treg total gene-signature for all the tumor types we analyzed **(Figure S5**). In line with poor survival associated with the presence of Itgb8 Tregs in the TME of patients, we observed that the expression of *ITGB8* Treg signature in the TME was inversely corelated with the activation of CD8 T cells present in the same TME (Fig. 6B**).** Thus, these data suggest that *ITGB8* expression in Tregs present in the TME might be useful as predictor of poor patient survival and activation of CD8 T cells in tumors.

Moreover combined with our analysis in mice, the aforementioned observations suggest that neutralizing Itgb8 ability to activate TGF-b in patient tumors could be associated with stronger CD8 T cells activation in the TME.

Neutralization of Itgβ8 exacerbates cytotoxic T cell function in TME of patients

Finally, we assessed whether neutralizing Itgb8 ability to activate TGF-b in patient tumors could affect effector t cells ability to respond to TGF-b and develop efficient anti-tumor response in the TME. To this end, we used an *ex-vivo* culture approach in which two serial sections of live tumor were cultured either in the presence or in the absence of neutralizing anti-Itgβ8 antibody (Fig. 7A). This technique allowed us to address the effects of the anti-Itgb8 antibody on same TME of given same patient in which the immune system compartment and its interactions with the tumor tissues were conserved. After treatment, $CD8^{pos}$ T cells from the tumors were analyzed by flow cytometry (Fig. 7B). We first monitored the effects of the anti-Itgb8 antibody treatment on TGF-b signaling in patient melanoma. In response to anti-Itgβ8 antibody, we observed 30–50% of reduction in phosphorylation of SMAD2/3 in $CD8^{pos}$ T cells from TME demonstrating that neutralizing Itgβ8 in the human tumors affects the levels of TGF-β signaling in $CD8^{pos}$ T cells infiltrating the TME (Fig. 7C-D). Strikingly, we also observed a 2–5 fold-increase of cytotoxic features of $CD8^{pos}$ T cells present in the TME in the majority of the melanoma after anti-Itgβ8 antibody treatment compared to untreated condition (Fig. 7E-F**).** Of note, similar observations were made in breast cancers in response to neutralizing anti-Itgβ8 antibody treatment **(Figure S6**). Thus, neutralizing Itgβ8 is sufficient to impair TGF-β signaling in $CD8^{pos}$ T lymphocytes infiltrating human tumors and boost their cytotoxic functions, opening the path towards clinical applications based on Itgb8 targeting in cancer.

Discussion

The presence of Tregs in the TME is usually associated with a weakness of the effector T cell responses and poor prognosis in patients. Though Tregs do not need to produce their own TGF-β1 to repress the effector T cell functions in the TME [12], this study reveals that Tregs, and particularly the $Itgβ8^{pos}$ population, are essential to increase the levels of activated TGF-β produced by cancer cells responsible for an efficient repression of T cell cytotoxic functions within the TME. Thus, this collaborative work between cancer cells and $Itgβ8^{pos}$ Tregs increases the ability of the cancer cells to escape the immune system and fosters cancer progression.

In certain cancers, *Itgb8* expression is observed in tumor cells express and the forced expression of *Itgb8* in cancer cell lines was associated with TGF-b1 activation *in vitro* as well as the impairment of metastasis growth and vascularization modifications of the tumors after their implantation in mice [23]. Our results do not exclude other cellular actors than $Itgβ8^{pos}$ Tregs participate to TGF-b activation in the TME. Indeed, we observed that TGF-b signaling in T cells infiltrating the tumors is not fully abolished in $Foxp3^{\Delta Itgβ8}$ mice. However, no role of $Itgb8^{pos}$ cancer cells have been assigned to the regulation of the

CD8 T cell cytotoxic functions in the TME[23]. Hence, we propose that once Itgb8^{pos} Tregs colonize the tumor, they help enforce the activation of latent TGF-b1 produced by cancer cells so far ensured by others cells of the TME, including cancer cells themselves in the tumors where they express αvβ8 integrin. This help from the Tregs allows the TME to reach the optimal activation of TGF-β1 which block the cytotoxic functions of CD8 T cells and promote tumor immune escape. The control of TGF-b signaling in CD8 T cells by activating TGF-b1 is likely facilitated by the unique ability of Tregs to be in the close vicinity of CD8 T cells in the TME [24]. The ability of Itgβ8^{pos} Tregs to activate TGF-β1 produced by cancer cells is in agreement with recent biochemical investigations on αvβ8-mediated TGF-β1 activation, made outside the Treg context, suggesting that the latent complex released by a given cell can be activated by αvβ8 integrin expressed by others [25]. Moreover, Tregs have been shown to be capable of acquiring at their surface latent complex produced by other cells [26].

Interestingly, the capacity of Itgβ8^{pos} Tregs to increase the levels of bioactive TGF-β1, to ensure a repression of the cytotoxic functions of T cells appears particularly of importance in the TME. Indeed, in clear contrast to the TME, the absence of Itgβ8 expression in Tregs failed to alter TGF-β signaling in effector T cells in the tdLN, implying that either other cells expressing Itgβ8 or other mechanisms, independent of the Itgβ8, play a key role in the activation of TGF-β in the secondary lymphoid organs. In line with this, while a modification on LAP of the RGD sequence recognized by avb8 integrin recapitulates the autoimmune syndromes observed in the absence of TGF-β1 [14], no signs of autoimmunity nor immune disorders were described in Foxp3$^{\Delta Itg\beta 8}$ mice, [17, 18]. Moreover, depending of the tissue, the predominant role of certain cells have been depicted in the activation of TGF-b. In the gut, Itgβ8^{pos} dendritic cells appear as key activators of TGF-β, whereas in the skin this function seems to be more dependent on keratinocytes [27, 28 29]. In addition, the inflammatory context favors the role of Itgβ8^{pos} Tregs in activating latent TGF-b [18]. Whether some inflammatory factors present in the TME reduce the expression of Itgβ8 by other cells than Tregs or repress alternative mechanisms of TGF-β activation could be considered as suggested in the gut [30].

Secreted latent complex can be stored in the micro-environment of the secreting cells and thus be accessible to integrins [31]. Our data reveal that cancer cells as a major source of latent TGF-β complex stored in the TME which is activated by Itgβ8^{pos} Tregs. However, we do not exclude that Itgβ8^{pos} Tregs can also activate TGF-β once secreted. Indeed, one of the features of Tregs is to express at their surface high amounts of the protein GARP, which can bind latent complex, then present it to αvβ8 integrin and thus contribute to the activation of secreted latent TGF-β [26], [32]. However, in contrast to the absence of *Itgb8*, the deletion in Tregs of *Irrc32*, which encodes for GARP, is not sufficient to affect tumor growth [33]. While GARP expression on Tregs contributes to the activation of secreted latent complexes, that of Itgβ8 contributes to the activation of latent complexes stored in the TME. Since much of the secreted latent complex of TGF-b is stored in the tissue [31], this could explain why the absence of Itgβ8 expression in Tregs, and not that of GARP, is sufficient to influence TGF-b signal given to effector T cells and repress tumor-growth.

TGF-b signaling is known to directly affect the CD8 T cell cytotoxic function[8]. This study reveals that the activation of the latent complex by Itgβ8^{pos} Tregs directly influences the levels of TGF-β signaling delivered to intra-tumor effector CD8 T cells and thus their cytotoxic function. The restoration of TGF-β signaling in effector T cells fully prevents their cytotoxic functions associated with the deletion of Itgβ8 on Tregs and it confirms that the modulation of TGF-b signaling in effector cells by Itgβ8^{pos} Tregs as the main mechanisms of action this regulatory subset in the TME. Based on several observations made *in vitro* and in the gut TGF-β has been proposed to promote the conversion Foxp3^{neg} T cells towards Foxp3^{pos} cells in the tumor [34]. Interestingly, in the absence of Itgβ8^{pos}Tregs, the proportion and the numbers of Tregs remained unchanged within the TME. Moreover, the lack of *Tgfβ1* in cancer cells, which leads to the activate the cytotoxic function of CD8 T cells in the TME, failed to affect Treg homeostasis in the tumor. Hence, further investigations should confirm the ability of the activated TGF-b1 present in the TME to influence T effector cell conversion into Tregs.

Targeting TGF-b effects on the immune cells in the TME is a important field of investigation for numerous companies. Our data strongly suggest that targeting Itgb8 in patient could lead to potent activation the T cell cytotoxic program in the TME and control of the tumor progression. This idea is comforted by our ex-vivo experiments, revealing that anti-Itgb8 antibody treatment impairs TGF-b signaling in effector T cells and is sufficient to boost their cytotoxic functions in the TME of patients. Though the best way to efficiently target Itgb8 effects in patients need to define, the exacerbation of the cytotoxic functions of T lymphocytes selectively in the TME suggests that targeting Itgβ8^{pos} Tregs may represent a promising immunotherapy avoiding the risk of unleashing massive auto-immunity following a systemic neutralization of TGF-b effects [10].

In sum, this study reveals an unsuspected collaborative mechanism between cancer cells and Tregs with direct consequences on the repression of the anti-tumor function of effector T cells in tumors. Moreover, it provides evidence that targeting Itgβ8 could constitute a promising future anti-cancer immunotherapy in patients.

Experimental Procedures

Mice

Itgb8-td-Tomato mice were generated as described [16]. Generated animals were cross on *FOXP3-IRES-GFP* background [35] to follow Tregs. *FOXP3-Cre^{eYFP};Itgβ8$^{-/-}$* (Foxp3^{Ctrl}) mice *FOXP3-Cre^{eYFP};Itgβ8$^{fl/fl}$* (Foxp3$^{\Delta Itgβ8}$) mice [18], *CD4-Cre;Stop$^{fl/fl}$;tgfbr1^{CA};Foxp3^{GFP}* mice [19] were used.. C57BL/6 mice and CD57BL/6 CD3ε^{KO} (CD3^{KO}) mice were purchased (Charles Rivers, France). Importantly, though Itgβ8 is mainly expressed in Tregs, we validated any leakiness of *Foxp3-CRE* construct in Foxp3$^{\Delta Itgβ8}$ mice, by breading animals on Rosa26 reported background [36]. All animals were between 2–6 months of age, all on a C57BL/6 background. Mice were maintained in AniCan SPF mouse facility Lyon, France.

Patient tumors and anti-Itgβ8 antibody treatment

Primary breast adenocarcinoma tumors and primary melanoma were obtained by the Biological Resource Center of Centre Léon Bérard and Hospital Lyon Sud respectively. Primary melanoma, at non-invasive stages, were obtained after surgery in different regions of the body. Primary breast tumors, irrelevant of their hormonal status, were analyzed. No gender (melanoma) and age (breast cancer and melanoma) selection was performed to establish the patient cohort. Importantly, patients never received anti-cancer treatments prior surgery. Fresh tumors were treated by the Ex-vivo facility of the Centre Léon Bérard Lyon France. They were imbedded in the Ex-vivo facility specific matrix gel© and cut at 250 µm with microtome (Seica). Tumor slides were then cultured on Uvac 1264 in RPMI-completed medium, 1% FCS, 1% HEPES, 1% penicillin/streptomycin, 1% MEM-NEAA (LifeTechnologies), 1% NaPyruvate (LifeTechnologies) with 20µg/ml of neutralizing Itgβ8 antibody ADWA-16 provided by Dean Sheppard. Tumor slices were harvested 48 hours later, minced with scalpel, and incubated with 5 mg/ml collagenase IV (Gibco) and 1 mg/ml DNase I (Sigma, 11284932001) in RPMI supplemented with 1% FCS and 1% HEPES for 30 minutes at 37°C with agitation prior cytometer analysis.

Ethics

Experiments on mice were performed in accordance with the animal care guidelines of the European Union, ARRIVE guide line and French laws and were validated by the local Animal Ethic Evaluation Committee (#9239 and #19584). Patient tumors were obtained after approval of the protocol by the institutional review board and ethics committee, with fully informed patient consent (French agreement number: AC-2013-1871).

Cell lines

Breast medullary adenocarcinoma cell line E0771 and melanoma B16-F10 (B16) were obtained from ATCC. B16-shTGF-β1 cells were generated by introduction of shTGF-β1 RNA in B16. Briefly, lentiviral vectors encoding shRNA pLKO.1 puro *Tgf-β1*: NM-011577.1-1753s1c1 and empty vectors were kindly given by Prof. D. Klatzmann (Paris). Infected B16 were selected on puromycin (Sigma, P8833). MLEC cells, with luciferase activity reporting TGF-β signaling were previously described [37]. All cell lines were maintained in DMEM (Gibco, 31966-021) supplemented with 10% FCS (LifeTechnologies, 10270-106), 1% HEPES (LifeTechnologies, 15630-056), 1% penicillin/streptomycin (LifeTechnologies, 15140-122). 250 µg/ml of geneticin (LifeTechnologies, 10131-027) or 5 µg/ml of puromycin (P8833-10MG) were added for MLEC and B16-shTGF-β1 cell culture respectively. All cell lines were tested negative for mouse pathogens, including mycoplasma by PRIA test (Charles-Rivers).

Measure of active TGF-β

MLEC cells, with luciferase activity reporting TGF-β signaling [37] were incubated with Itgβ8^{neg} or Itgβ8^{pos} Tregs. Luciferase activity was detected via the Luciferase Assay System (Promega, E1500) on a TECAN. TGF-β bioactivity is presented in arbitrary units (A.U.) after withdrawal of blank value of medium alone.

Mouse tumor implantation and tissue preparation

5x10^5 B16 cells were injected intra-dermally (id) in the back skin. 5x10^5 E0771 cells were injected in the abdominal mammary gland # IV. Tumor growth was monitored every 3 days with caliper in double bind

manner. Tumor size (mm^3) was calculated as width x length x width. Tumors were minced with scalpel, and digested with 1 mg/ml collagenase IV (Sigma, C2674-1G) and DNAse I at 1 mg/ml (Sigma, 11284932001) in DMEM supplemented with 1% FCS and 1% HEPES. Tumor draining lymph nodes (tdLN, inguinal) were mechanically grinded with glass slides.

Adoptive T cell transfers

$Foxp3^{neg}CD3^{pos}$ cells from the lymph nodes of *CD4-Cre;Stop$^{fl/fl}$;tgfbr1^{CA};Foxp3^{GFP}*mice, *CD4-Cre;Foxp3^{GFP}*mice and $CD4^{pos}Foxp3^{pos}$ cells from $Foxp3^{Ctrl}$ and $Foxp3^{\Delta Itg\beta 8}$ were purified by cell sorting with ARIA-II (BD). $5x10^4$ $CD4^{pos}Foxp3^{pos}$ cells mixed with $4.5x10^5$ $CD3^{pos}Foxp3^{neg}$ were intravenously injected to $CD3\varepsilon^{KO}$ mice.

$CD8^{pos}$ T cell depletion

Depletion of $CD8^{pos}$ T cells was performed by intra-peritoneal injection of anti-CD8β (BioXCell, clone Lyt3.2; BE0223). 150 µg per mouse were injected four days prior tumor injection and every four days all along the experiment. Depletion was systematically checked by flow cytometry on blood samples before tumor injection and on lymph nodes and on the tumors after the experiments using a different anti-CD8β clone (YTS156.7.7, Biolegend).

Cell sorting and flow cytometry analysis

Surface staining of mouse cells was performed using the following fluorescent-conjugated antibodies: CD3ε (145-2C11; BD biosciences), CD4 (RM4-5; Biolegend), CD8α (53.6.7; BD biosciences), CD45 (30-F11; BD biosciences), CD107a (eBio1D4B, eBiosciences). For intracellular staining cells were fixed and permeabilized using Fixation and Permeabilization Buffer kit (00-5523-00, eBiosciences) according to the manufacturer's protocol. Granzyme B (GRB05 Invitrogen), Ki67 SolA15; ThermoFisher were used. For cytokine staining cells were incubated with brefeldin A (eBioscience), for four hours, IFN-γ (XMG1.2 BD bioscience) staining was performed with Buffer kit (00-5523-00, eBiosciences). For p-SMAD2/3 staining, cells were immediately fixed with Fixation and Permeabilization Buffer kit (00-5523-00 eBiosciences) prior staining and anti-p-SMAD2/3 (D27F4, Cell Signaling) was detected with goat anti-rabbit A488 (LifeTechnologies, A11034). For cell sorting, T-cells were enriched with Pan T cell isolation kit II mouse (Miltenyi Biotec) and then stained with CD4 (GK1.5; ThermoFisher) and CD8 (53.6.7; BD biosciences). $Itg\beta 8\text{-td-Tomato}^{Pos}$ $Foxp3^{GFP}CD4^{pos}$ cells, $Itg\beta 8\text{-td-Tomato}^{neg}$ $Foxp3^{GFP}CD4^{pos}$ cells, $CD4^{pos}Foxp3\text{-}^{YFPpos}$ cells and $CD3^{pos}Foxp3^{YFPneg}$ cells were sorted on FACS ARIA II. Human cell stainings were performed using the following fluorescent-conjugated antibodies: CD3 (UCHT1; BD biosciences), CD45 (HI30; BD biosciences), CD4 (RPA-T4; LifeTechnologies), CD8 (SK1; BD biosciences), CD107a (H4A3; BD biosciences) and Granzyme B (GRB05 Invitrogen) p-SMAD2/3 (D27F4, Cell Signaling). All samples were acquired on BD Fortessa and data were analyzed with FlowJo Software version X.

Mouse tumor TUNEL and immune-fluorescence staining

Tumor were embedded in Tissue tek OCT compound (Sakura Finetek) and snap-frozen; 10 µm thick sections were cut with CryoStar NX50 (Microm Microtech France). For TUNEL staining, sections were

permeabilized with 0.2% Triton (Sigma, T9284) and digested with Proteinase K (ThermoFisher, K182001). For positive control, sections were incubated with DNAse I at 1mg/ml (Sigma, 11284932001). Sections were then incubated with biotin-16-dUTP (Sigma, 11093070910) and TUNEL enzyme (Sigma, 11767305001) in deoxynucleotidyltransferase buffer (1mM CoCl2 (Sigma, 15862-1ml-F), Tris-HCl, 200mM Sodium Cacodylate (Sigma, C0250-25G), 0.125% BSA (Sigma, A7906-500G)) at 37°C for 60 min. Sections were washed in stop buffer (300mM NaCl (Sigma, S3014-1KG), 30mM Sodium Citrate (Sigma, 71406-500G)) and blocked with 2% BSA. Sections were then labelled with streptavidin-Phycoerythrin (eBiosciences, 12-4317-87), CD8-A488 (53 – 6.7, BD biosciences). For immunostaining, tumor sections were fixed in 4% PFA (Sigma) and stained with rabbit anti-mouse GP100 (ab137078 Abcam) and or LAP-PE (TW7-16B4, Biolegend). All sections were stained with DAPI (Euromedex, 1050-A) and mounted with Fluoromount (Sigma, F4680-25ml). All samples were acquired on Upright microscope Zeiss Axioimager (SIP 60549) and data were analyzed with Zen 2 (blue edition).

Quantitative real-time PCR

mRNAs were isolated with RNeasy mini kit (Qiagen) and reverse transcribed with iScript cDNA synthesis kit (Biorad). Real-time RT-PCR was performed using LightCycler 480 SYBR Green Master (Roche) and different set of primer on Light Cycler 480 Real-Time PCR System (Roche). Samples were normalized on GAPDH and analyzed according to the $\Delta\Delta$Ct method.

Primers	Sequence 5’ ◊ 3’
mTGF-β1 (forward)	ATCCTGTCCAAACTAAGGCTCG
mTGF-β1 (reverse)	ACCTCTTTAGCATAGTAGTCCGC
GAPDH (forward)	AGGTCGGTGTAACGGATTTG
GAPDH (reverse)	TGTAGACCATGTAGTTGAGGTCA

Single Cell RNA-Seq analysis

Publicly available single cell data was used to infer a transcriptome signature of ITGB8-expressing T cells and Treg cells across different tumor types. scRNAseq counts were downloaded from the GEO repository for melanoma (SKCM: GSE115978), colorectal cancer (CCA: GSE108989), liver cancer (HCC: GSE98638), and non-small cell lung cancer (NSCLC: GSE99254). All single cell data was analyzed with the 'Seurat' package v.3.1.0 (Stuart et al., 2019). After creating a seurat object, the sctransform wrapper was used for normalization, scaling, and identification of variable features within each dataset. UMAP projections were used for visualization of expression and co-expression patterns. The "FindMarkers" function was used with standard settings to identify genes differentially expressed in *ITGB8*^{pos} Tregs (CCA, HCC, and NSCLC). For each set of *ITGB8* single-cell markers, the singscore gene signature scoring method was used to score *ITGB8*^{pos} Treg activity (Foroutan M, Bhuva DD, Lyu R, Horan K, Cursons J, Davis MJ (2018). “Single sample scoring of molecular phenotypes.” BMC bioinformatics, 19(1), 404. doi: 10.1186/s12859-

018-2435-4). The singscore method uses rank-based statistics to analyze the sample's gene expression profile and scores the expression activities of gene sets at a single-sample level.

TCGA data exploitation

Melanoma (SKCM), colon cancer (COAD), liver cancer (LIHC) and lung cancer (LUAD) gene expression and clinical data was downloaded from the The Cancer Genome Atlas (TCGA) repository [https://www.cancer.gov/tcga.] using the R packages 'TCGAbiolinks' v.2.9.4 (Colaprico et al., 2016) and 'RTCGA.clinical' v.20151101.8.0 [Kosinski M (2019). RTCGA. clinical: Clinical datasets from The Cancer Genome Atlas Project. R package version 20151101.14.0.], respectively. Briefly, each dataset was queried for Illumina HiSeq RNA-Seq results. Downloaded data was preprocessed, normalized and filtered using 'TCGAbiolinks' and edgeR (Robinson MD, McCarthy DJ, Smyth GK (2010). “edgeR: a Bioconductor package for differential expression analysis of digital gene expression data.” Bioinformatics, 26(1), 139–140. doi: 10.1093/bioinformatics/btp616.), and a Itgb8^{pos} score was calculated for each sample, as described above. Tumor samples were classified into two groups, Low and High, based on the median of the Itgb8^{pos} score. Survival data (i.e. time to last follow-up and overall survival status), was used to fit a Cox proportional hazards regression model using the 'survival' package v.2.44–1.1 [https://CRAN.R-project.org/package=survival]. Survival Kaplan-Meier curves were plotted with 'survminer' v.0.4.5 [https://CRAN.R-project.org/package=survminer].Additional validations and score correlations were also performed in the melanoma expression dataset by Abril-Rodriguez et al. (https://doi.org/10.1038/s43018-019-0003-0).

Statistical analysis

Statistical analysis was performed using paired t-test, unpaired t-test, Mann-Whitney or Wilcoxon when appropriate. For survival analysis Mantel Cox proportional hazard model was used. Differences were considered significant when p values were < 0.05. Correlation score were obtained using Spearman test.

Declarations

Statistical analysis

Statistical analysis was performed using paired t-test, unpaired t-test, Mann-Whitney or Wilcoxon when appropriate. For survival analysis Mantel Cox proportional hazard model was used. Differences were considered significant when p values were < 0.05. Correlation score were obtained using Spearman test.

Acknowledgements

The expert assistance of V. Bernet and S Rodriguez is acknowledged as well as the advices and analysis from V. Fontanier. We also thank Drs S. Soudja and V. Dardalhon for critical comments and the Marie lab members for their helpful discussions. We thank Dr Bartholin for sharing TGFbRI^{CA} mice and Prof Ribas for sharing data on melanoma patients. This work was supported by grants from LabEx DEVweCAN ANR investissement d’Avenir ANR-10-LABX-61 (JCM), the Helmholtz-DKFZ-Inserm program (JCM), BMS foundation Grant, and Foncer contre le cancer, ARC grant # 2019-1047, the labelisation ligue Nationale

contre cancer (JCM). Agence Nationale de la Recherche ANR-13-PDOC-0019 (HP) and People Program (Marie Sklodowska-Curie Actions) of the European Union (PIIF-GA-2012-330432) (HP). A.L was supported by a LabEx DEVweCAN grant and Ligue Nationale Contre le Cancer. OL was supported by the Ligue Nationale Contre le Cancer and ST by a PhD fellowship from the French Ministry of Higher Education. The SIRIC LYriCAN INCa-DGOS-Inserm_12563 is acknowledged.

Author contributions: A.L, O.L, and J.C.M planned, conducted experiments and analyzed data. H.H-V performed bio-informatic analysis. S.T and H.P generated the Itgb8-dt-Tomato mice. S.L A.L and O.L performed patient-tumor ex-vivo cultures and A.S tumor-cell injections and double-blind tumor measurements. D.S provided the anti-Itgb8 antibody, S.D. patient melanoma and M.A.T Itgb8$^{fl/fl}$ mice. J.C.M and A.L wrote the manuscript. H.P and M.A.T performed comments and corrections. J.C.M supervised the study.

Competing interests: The authors declare that they have no competing interests.

References

1. Batlle, E. & Massague, J. Transforming Growth Factor-beta Signaling in Immunity and Cancer. *Immunity* **50**, 924–940 (2019).
2. Cerami, E. *et al.* The cBio cancer genomics portal: an open platform for exploring multidimensional cancer genomics data. *Cancer Discov* **2**, 401–404 (2012).
3. Gao, J. *et al.* Integrative analysis of complex cancer genomics and clinical profiles using the cBioPortal. *Sci Signal* **6**, pl1 (2013).
4. Shull, M.M. *et al.* Targeted disruption of the mouse transforming growth factor-beta 1 gene results in multifocal inflammatory disease. *Nature* **359**, 693–699 (1992).
5. Marie, J.C., Liggitt, D. & Rudensky, A.Y. Cellular mechanisms of fatal early-onset autoimmunity in mice with the T cell-specific targeting of transforming growth factor-beta receptor. *Immunity* **25**, 441–454 (2006).
6. Li, M.O., Sanjabi, S. & Flavell, R.A. Transforming growth factor-beta controls development, homeostasis, and tolerance of T cells by regulatory T cell-dependent and -independent mechanisms. *Immunity* **25**, 455–471 (2006).
7. Gorelik, L. & Flavell, R.A. Immune-mediated eradication of tumors through the blockade of transforming growth factor-beta signaling in T cells. *Nat Med* **7**, 1118–1122 (2001).
8. Thomas, D.A. & Massague, J. TGF-beta directly targets cytotoxic T cell functions during tumor evasion of immune surveillance. *Cancer Cell* **8**, 369–380 (2005).
9. Dahmani, A. & Delisle, J.S. TGF-beta in T Cell Biology: Implications for Cancer Immunotherapy. *Cancers (Basel)* **10** (2018).
10. Huynh, L.K., Hipolito, C.J. & Ten Dijke, P. A Perspective on the Development of TGF-beta Inhibitors for Cancer Treatment. *Biomolecules* **9** (2019).

11. Travis, M.A. & Sheppard, D. TGF-beta activation and function in immunity. *Annu Rev Immunol* **32**, 51–82 (2013).
12. Donkor, M.K. *et al.* T cell surveillance of oncogene-induced prostate cancer is impeded by T cell-derived TGF-beta1 cytokine. *Immunity* **35**, 123–134 (2011).
13. Courau, T. *et al.* TGF-beta and VEGF cooperatively control the immunotolerant tumor environment and the efficacy of cancer immunotherapies. *JCI Insight* **1**, e85974 (2016).
14. Yang, Z. *et al.* Absence of integrin-mediated TGFbeta1 activation in vivo recapitulates the phenotype of TGFbeta1-null mice. *J Cell Biol* **176**, 787–793 (2007).
15. Aluwihare, P. *et al.* Mice that lack activity of alphavbeta6- and alphavbeta8-integrins reproduce the abnormalities of Tgfb1- and Tgfb3-null mice. *J Cell Sci* **122**, 227–232 (2009).
16. Nakawesi, J. *et al.* alphavbeta8 integrin-expression by BATF3-dependent dendritic cells facilitates early IgA responses to Rotavirus. *Mucosal Immunol* (2020).
17. Edwards, J.P., Thornton, A.M. & Shevach, E.M. Release of active TGF-beta1 from the latent TGF-beta1/GARP complex on T regulatory cells is mediated by integrin beta8. *J Immunol* **193**, 2843–2849 (2014).
18. Worthington, J.J. *et al.* Integrin alphavbeta8-Mediated TGF-beta Activation by Effector Regulatory T Cells Is Essential for Suppression of T-Cell-Mediated Inflammation. *Immunity* **42**, 903–915 (2015).
19. Doisne, J.M. *et al.* iNKT cell development is orchestrated by different branches of TGF-beta signaling. *J Exp Med* **206**, 1365–1378 (2009).
20. Bartholin, L. *et al.* Generation of mice with conditionally activated transforming growth factor beta signaling through the TbetaRI/ALK5 receptor. *Genesis* **46**, 724–731 (2008).
21. Long, A.G., Lundsmith, E.T. & Hamilton, K.E. Inflammation and Colorectal Cancer. *Curr Colorectal Cancer Rep* **13**, 341–351 (2017).
22. Plitas, G. *et al.* Regulatory T Cells Exhibit Distinct Features in Human Breast Cancer. *Immunity* **45**, 1122–1134 (2016).
23. Takasaka, N. *et al.* Integrin alphavbeta8-expressing tumor cells evade host immunity by regulating TGF-beta activation in immune cells. *JCI Insight* **3** (2018).
24. Curiel, T.J. *et al.* Specific recruitment of regulatory T cells in ovarian carcinoma fosters immune privilege and predicts reduced survival. *Nat Med* **10**, 942–949 (2004).
25. Campbell, M.G. *et al.* Cryo-EM Reveals Integrin-Mediated TGF-beta Activation without Release from Latent TGF-beta. *Cell* **180**, 490–501 e416 (2020).
26. Tran, D.Q. *et al.* GARP (LRRC32) is essential for the surface expression of latent TGF-beta on platelets and activated FOXP3 + regulatory T cells. *Proc Natl Acad Sci U S A* **106**, 13445–13450 (2009).
27. Travis, M.A. *et al.* Loss of integrin alpha(v)beta8 on dendritic cells causes autoimmunity and colitis in mice. *Nature* **449**, 361–365 (2007).

28. Hirai, T. *et al.* Keratinocyte-Mediated Activation of the Cytokine TGF-beta Maintains Skin Recirculating Memory CD8(+) T Cells. *Immunity* **50**, 1249–1261 e1245 (2019).
29. Worthington, J.J., Czajkowska, B.I., Melton, A.C. & Travis, M.A. Intestinal dendritic cells specialize to activate transforming growth factor-beta and induce Foxp3 + regulatory T cells via integrin alphavbeta8. *Gastroenterology* **141**, 1802–1812 (2011).
30. Chanab, D., Boucard-Jourdin, M. & Paidassi, H. Gut Inflammation in Mice Leads to Reduction in alphavbeta8 Integrin Expression on CD103 + CD11b- Dendritic Cells. *J Crohns Colitis* **11**, 258–259 (2017).
31. Hinz, B. The extracellular matrix and transforming growth factor-beta1: Tale of a strained relationship. *Matrix Biol* **47**, 54–65 (2015).
32. Lienart, S. *et al.* Structural basis of latent TGF-beta1 presentation and activation by GARP on human regulatory T cells. *Science* **362**, 952–956 (2018).
33. Vermeersch, E. *et al.* Deletion of GARP on mouse regulatory T cells is not sufficient to inhibit the growth of transplanted tumors. *Cell Immunol* **332**, 129–133 (2018).
34. Maruyama, T., Konkel, J.E., Zamarron, B.F. & Chen, W. The molecular mechanisms of Foxp3 gene regulation. *Semin Immunol* **23**, 418–423 (2011).
35. Wang, Y. *et al.* Th2 lymphoproliferative disorder of LatY136F mutant mice unfolds independently of TCR-MHC engagement and is insensitive to the action of Foxp3 + regulatory T cells. *J Immunol* **180**, 1565–1575 (2008).
36. Srinivas, S. *et al.* Cre reporter strains produced by targeted insertion of EYFP and ECFP into the ROSA26 locus. *BMC Dev Biol* **1**, 4 (2001).
37. Abe, M. *et al.* An assay for transforming growth factor-beta using cells transfected with a plasminogen activator inhibitor-1 promoter-luciferase construct. *Anal Biochem* **216**, 276–284 (1994).

Figures

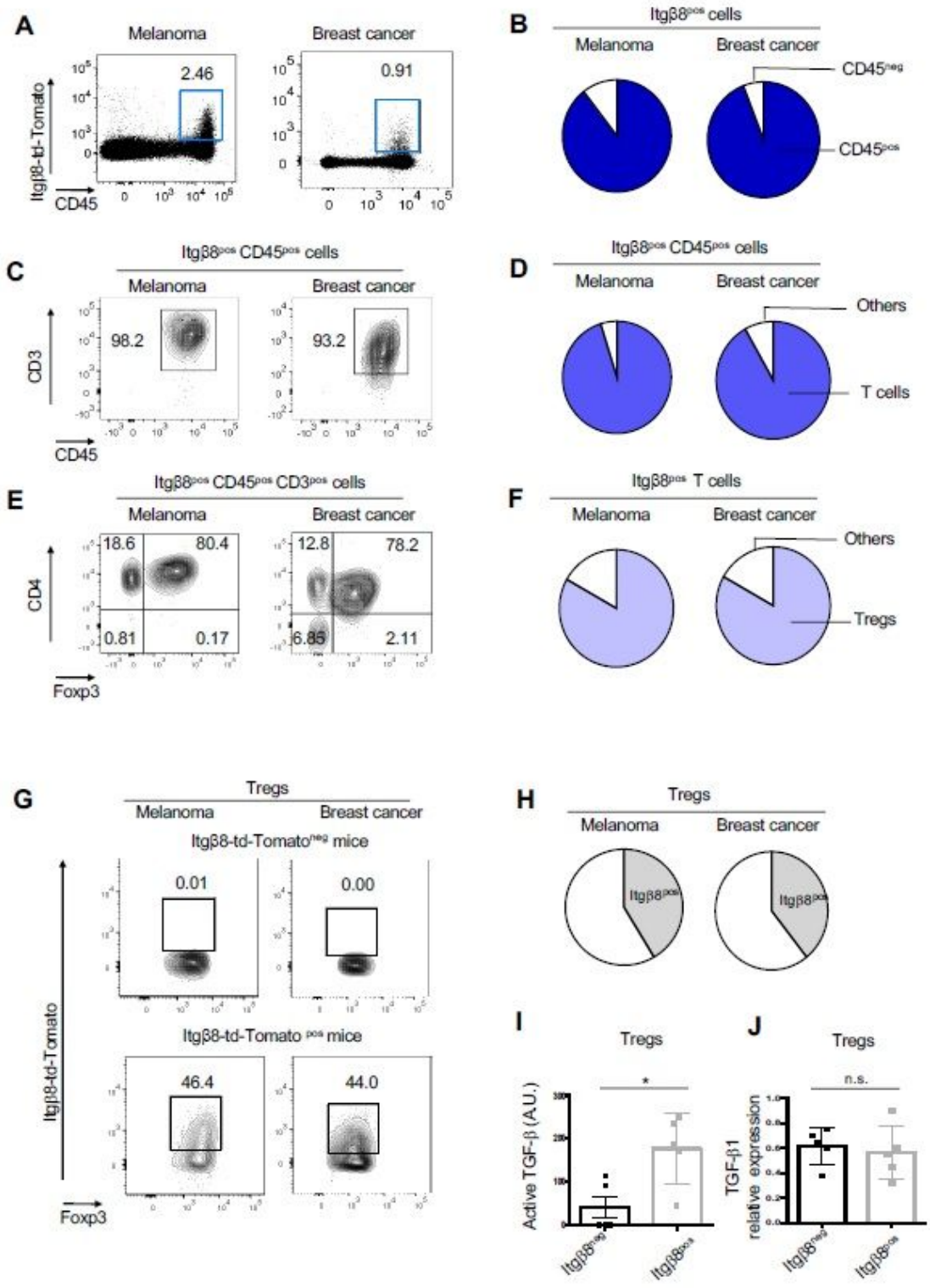

Figure 1

Tregs compose the main cells expressing Itgb8 in tumors. Itgb8-td-Tomato reporter mice were injected with melanoma cells (B16) or breast cancer cells (E0771) in the dermis or in the mammary gland respectively. 18 days later tumors were analyzed by flow cytometry. Percentages of the gated populations are mentioned on dot plots and counter plots. A) Representative plots illustrate the Itgb8-tdTomato expression in tumors. B) Pie-charts demonstrating the percentages of Itgb8pos cells among the

hematopoietic compartment (CD45pos) and the non-hematopoietic compartment (CD45neg). C, E) Representative contour plots illustrating the proportion of CD3pos cells among Itgb8-td-Tomatopos CD45pos cells and CD4pos Foxp3pos (Tregs) among Itgb8-td-Tomatopos T cells. D-F) Pie-charts represent the average percentage of T cells among the Itgb8-tdTomatopos CD45pos cells and the percentage Tregs among the Itgb8-tdTomatopos T cells in 3-5 tumors of each. G) Representative contour plots illustrating the Itgb8-tdTomato expression in Foxp3pos CD4pos T cells. H) Pie-chart illustrates the average percentage of Tregs expressing Itgb8-tdTomato from 3-5 tumors of each. I-J) Itgb8-tdTomatopos Tregs and Itgb8-tdTomatoneg Tregs were FACS-sorted, and their ability to activate TGF-b using TGF-b signaling reporter cells was measure I, as well as their ability to express Tgfb1 by RTqPCR. Graphs illustrate the levels of bio-activated TGF-b expressed in arbitrary unit (A.U.) (I), as well as the levels of expression Tgfb1mRNA normalized on Gadph. Error bar, mean ± SD. Data in I-J are representative of 2 experiments with 5 animals in total, each mouse providing both types of cells. * $p<0.05$ paired two-tailed Student's t test. ns: statistically not significant.

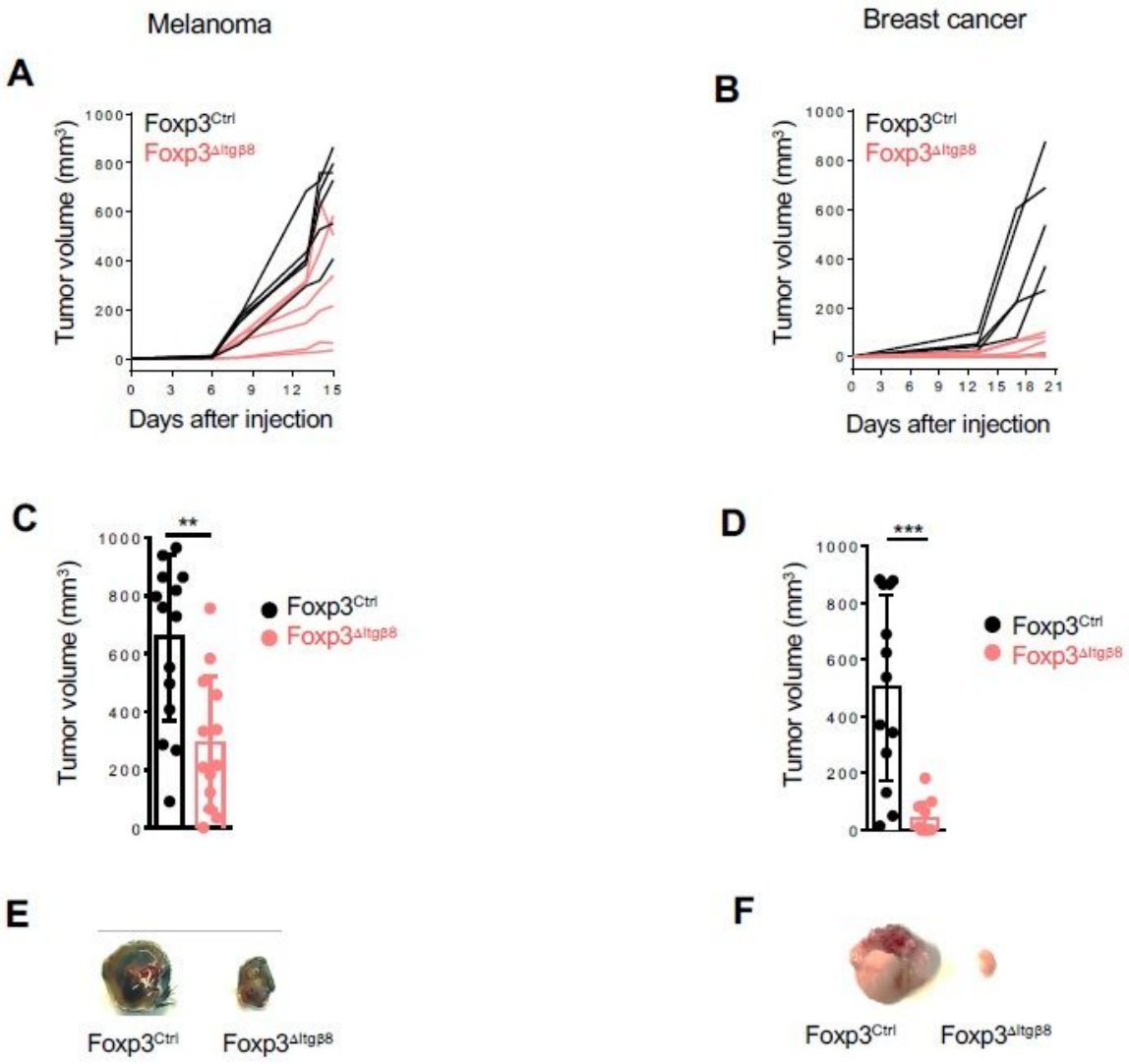

G

	Foxp3^{Ctrl}	Foxp3$^{\Delta Itg\beta 8}$
# of mice	16	16
# of mice with non-mesurable melanoma (%)	0 (0%)	4 (25%)

H

	Foxp3^{Ctrl}	Foxp3$^{\Delta Itg\beta 8}$
# of mice	16	16
# of mice with non-mesurable breast cancer (%)	1 (6.25%)	8 (50%)

Figure 2

Itgβ8 expression on Tregs promotes tumor growth. Foxp3DItgβ8 mice and their littermate controls (Foxp3Ctrl) were injected either i.d. with melanoma (B16 cells) or in the mammary gland with breast cancer (E0771 cells). A, B) Representative graphs illustrating the size of the tumors at different days post-injection. n = 5-8 mice per groups. Data representative of 2 independent experiments. C, D) Graphs demonstrate the tumor size (mean ± SD), at the day of the sacrifice (18 days after injections) of the 2 independent experiments with a total of 16 mice per groups. ***p < 0.001 and **p < 0.01 were determined

by unpaired Student t-test. E, F) Representative pictures of tumors at the end of the experiments. G, H) Table showing the percentage of Foxp3DItgβ8 mice and Foxp3WT mice with a completed control of tumor-growth (tumor < 100 mm3 all along the experiments) for both melanoma and breast cancer.

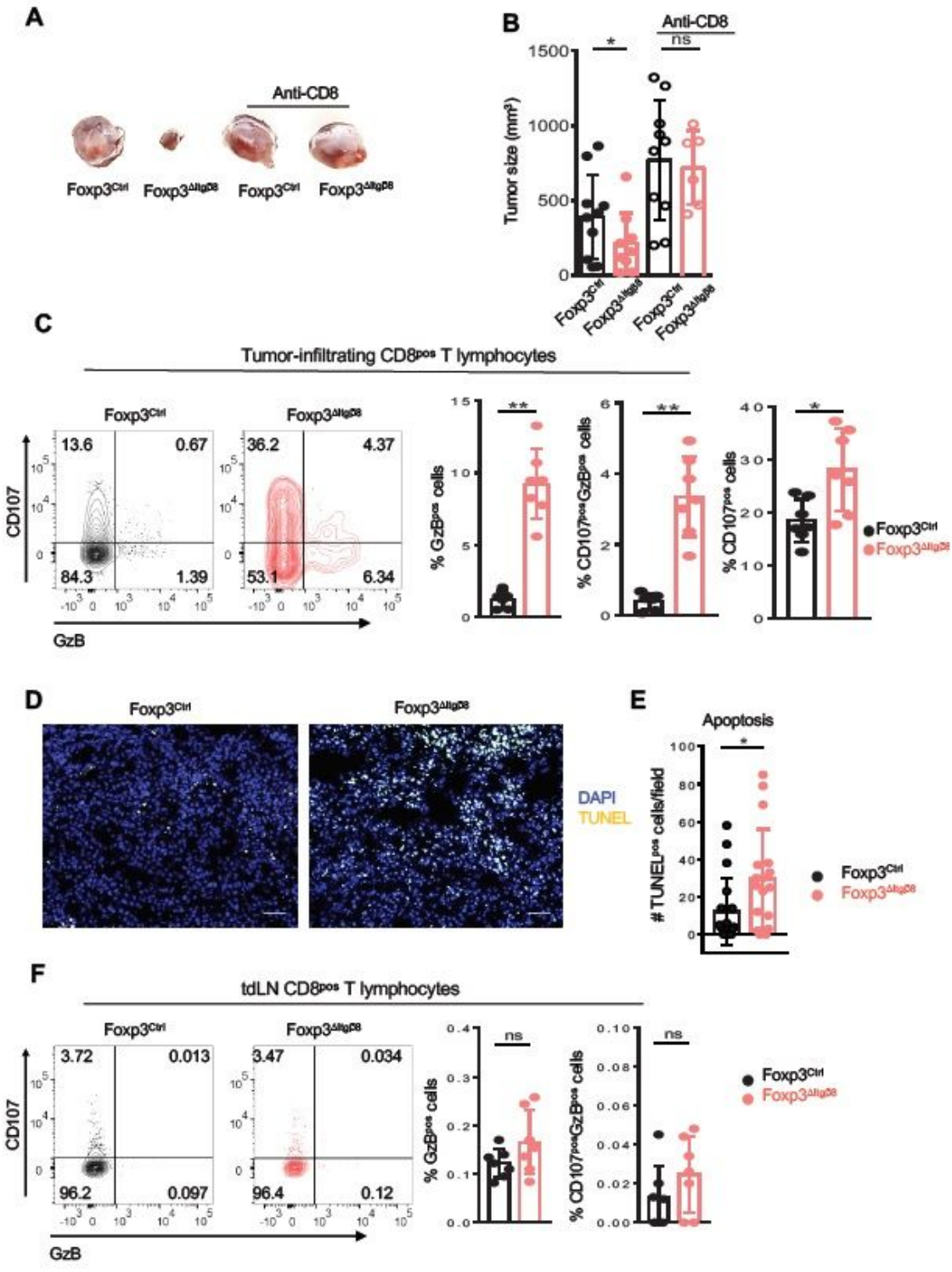

Figure 3

Itgβ8 expression in Tregs impairs cytotoxic functions of tumor CD8pos T cells. A-B) Foxp3Ctrl mice and Foxp3DItgβ8 animals were treated or not with depleting anti-CD8b to selectively remove CD8pos T cells.

Animals were then injected i.d. with B16 cells. Pictures of tumors are representative of 6-11 animals from 2 independent experiments and graph represents the tumor size at day 15 after tumor implantation. C-F) Foxp3DItgβ8 mice and their littermate controls (Foxp3Ctrl) were injected either i.d. with B16 cells and tumors and their draining lymph node (dtLN) were analyzed by flow cytometry 15 days later (C, F). Counter plots illustrate the ability of CD8 cells to produce granzyme B (GzB) and degranulate based on CD107 cell surface expression CD8pos T cells infiltrating the tumor. Percentages of the gated populations are mentioned on counter plots. Histograms demonstrate the percentage of CD8pos T cells expressing GzB or co-expressing GzB and CD107 in different animals (n=7) from 2 independent. D-E) Representative pictures demonstrate TUNEL positive cells (yellow nucleus), tumor slides were stained with DAPI (blue). Graph illustrates the density of apoptotic cells. Data are representative of 2 experiments, with 7-8 mice per group. Error bar, mean ± SD. ** $p<0.01$, * $p<0.05$; Paired Student t-test for B, Mann Whitney for C -F.

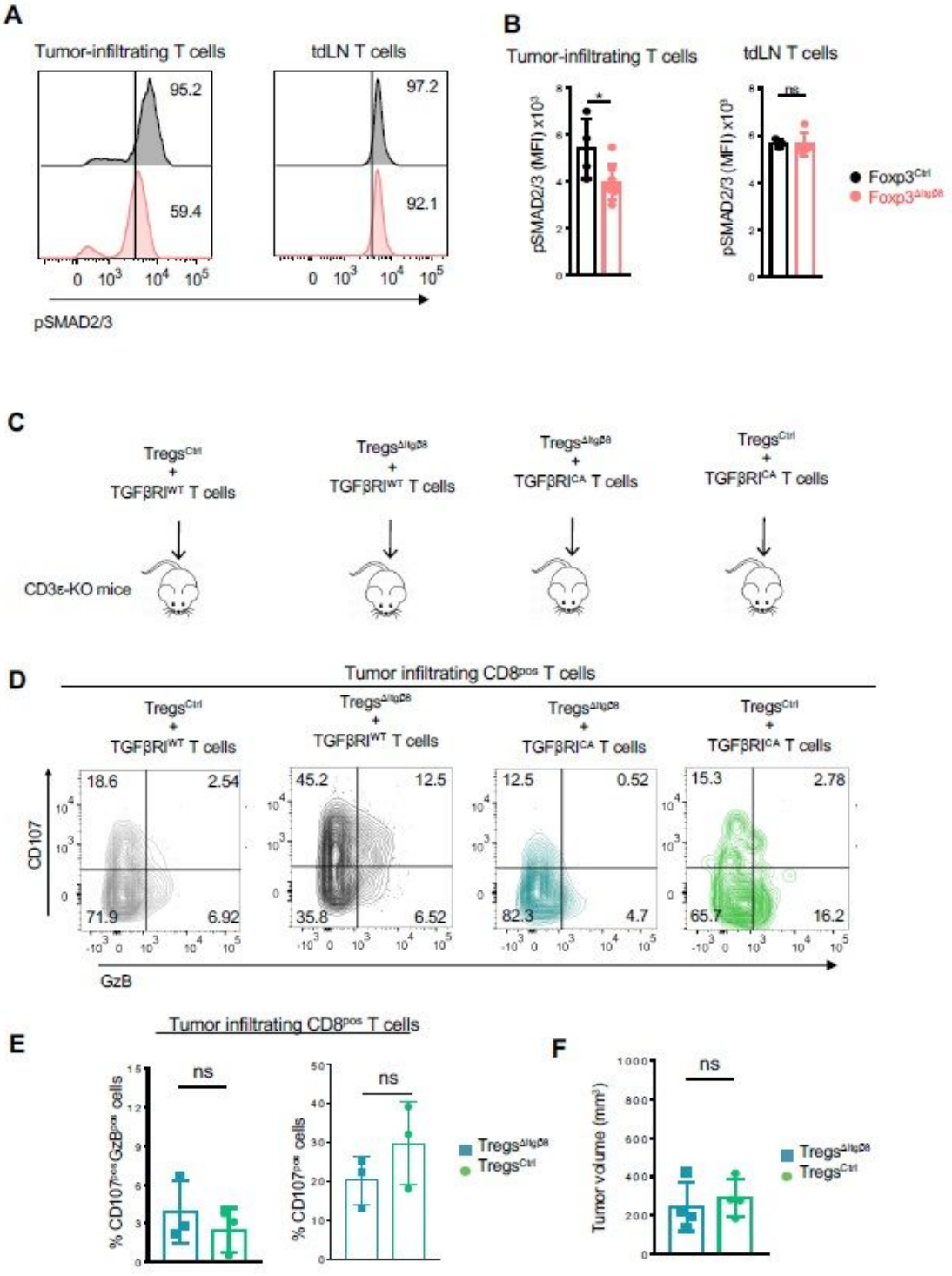

Figure 4

ltgβ8pos Tregs promote TGF-β signaling in intra-tumor T cells affecting their anti-tumor response. A-B) Foxp3Ctrl mice and Foxp3DItgβ8 animals were injected i.d. with B16 cells. Tumors and draining lymph nodes(tdLN) were harvested 15 days later and analyzed by flow cytometry. Representative histogram of the levels of phosphorylation of SMAD2/3 (pSMAD2/3) in tumor-infiltrating T cells (A) percentage of cells with high phosphorylation of SMAD2/3 are indicated on each histogram. Graphs demonstrate the mean

of fluorescence intensity (MFI) +SD in T cells (B). Data are representative of 2 independent experiments with 4-6 mice per group. C-E) Purified Tregs from either Foxp3Ctrl mice or Foxp3DItgβ8 mice were adoptively transferred with Foxp3neg T cells (CD3posGFPneg) from either CD4-Cre;Stopfl/fltgfbr1CA;Foxp3GFP mice (TGFbRICA) or their littermate controls (TGFbRIWT) in CD3εKO mice. 10 days later recipient mice were injected i.d. with B16 cells and their tumor analyzed 16 days after their implantation by flow cytometry. C) Representative contour plots of CD107 cell surface expression and GzB production by tumor-infiltrating CD8pos T cells are illustrated and percentages of each population mentioned populations on the counter plots. D) Graphs illustrate the percentage of GzBpos CD107pos cells and of CD107pos cells among CD8pos T cells infiltrating the tumors. E) Graph represents the tumor size at the end of the experiments. Data are representative of 2 independent experiments with 3-4 recipient mice per group. Means are shown ± SD. *$p < 0.05$, was determined by Mann-Whitney test. ns: statistically not significant.

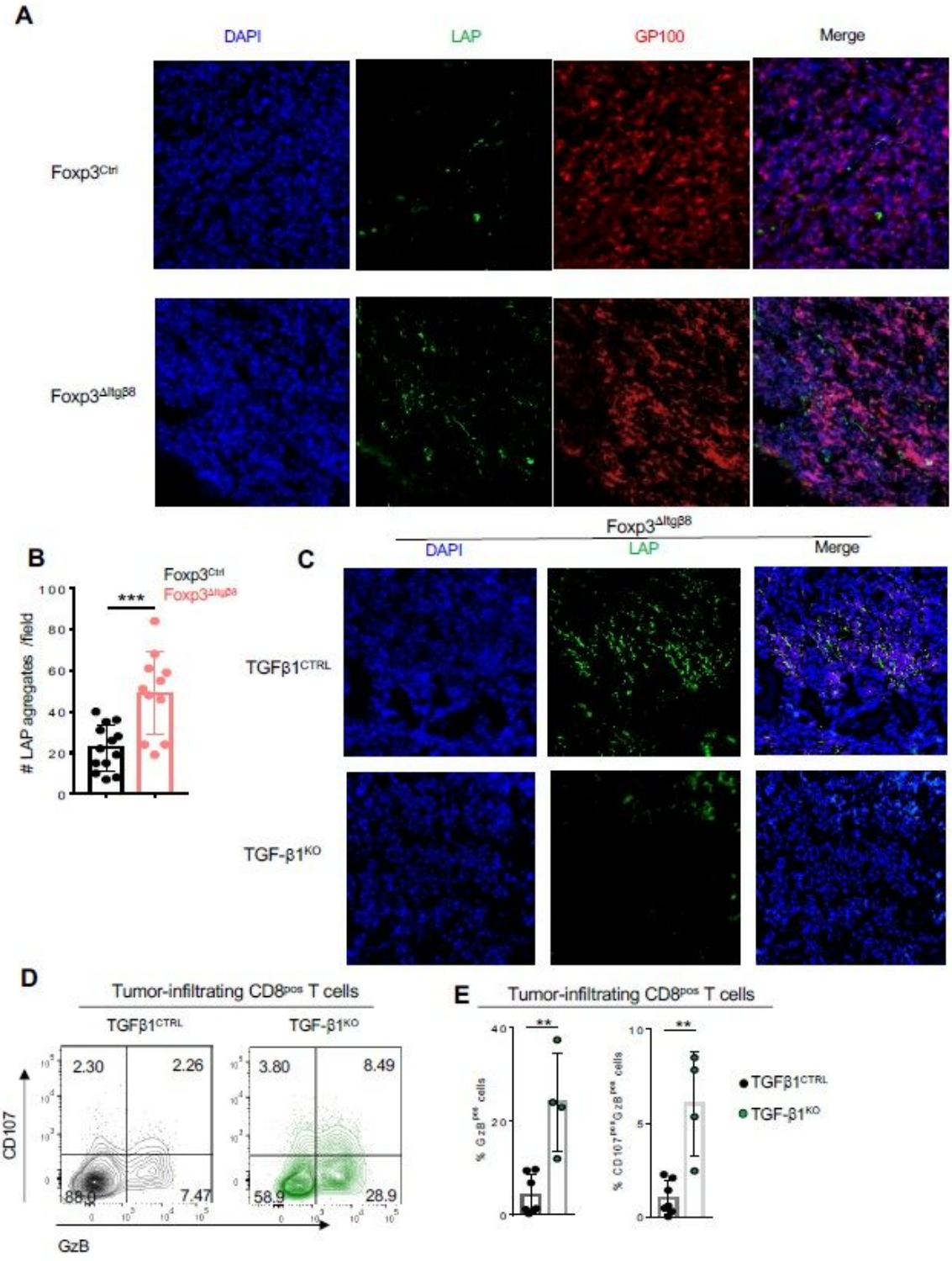

Figure 5

Itgb8pos Tregs activate TGF-b1 produced by cancer cells to repress tumor infiltrating CD8 T cells. A-B) Foxp3Ctrl mice and Foxp3DItgβ8 animals were injected i.d. with B16 cells. 15 days later tumors were harvested and analyzed by immunostaining for LAP and melanoma (GP100). Graph illustrates the numbers of LAP aggregates observed per field. C) Foxp3DItgβ8 animals were injected i.d. with either B16 shTgfb1 (TGFb1KO) or control B16 cells (TGFb1CTRL) or and tumors were harvested 15 days later and

analyzed by immunostaining for the presence of LAP aggregates. D-E) Foxp3Ctrl mice were injected i.d. with either TGFb1CTRL B16 cells or TGFb1KO B16 and CD8pos T cells infiltrating the tumors analyzed 15 days later flow cytometry. Representative counter plots illustrating the cytotoxic functions are shown as well as graphs demonstrating the percentage of CD8pos T cells expressing either granzyme B (GzB) or and GzB and CD107. means are shown ± SD. ***p < 0.001 was determined by unpaired Student t-test (B) and means are shown ± SD. **p < 0.01 was determined by Mann-Whitney test (E).

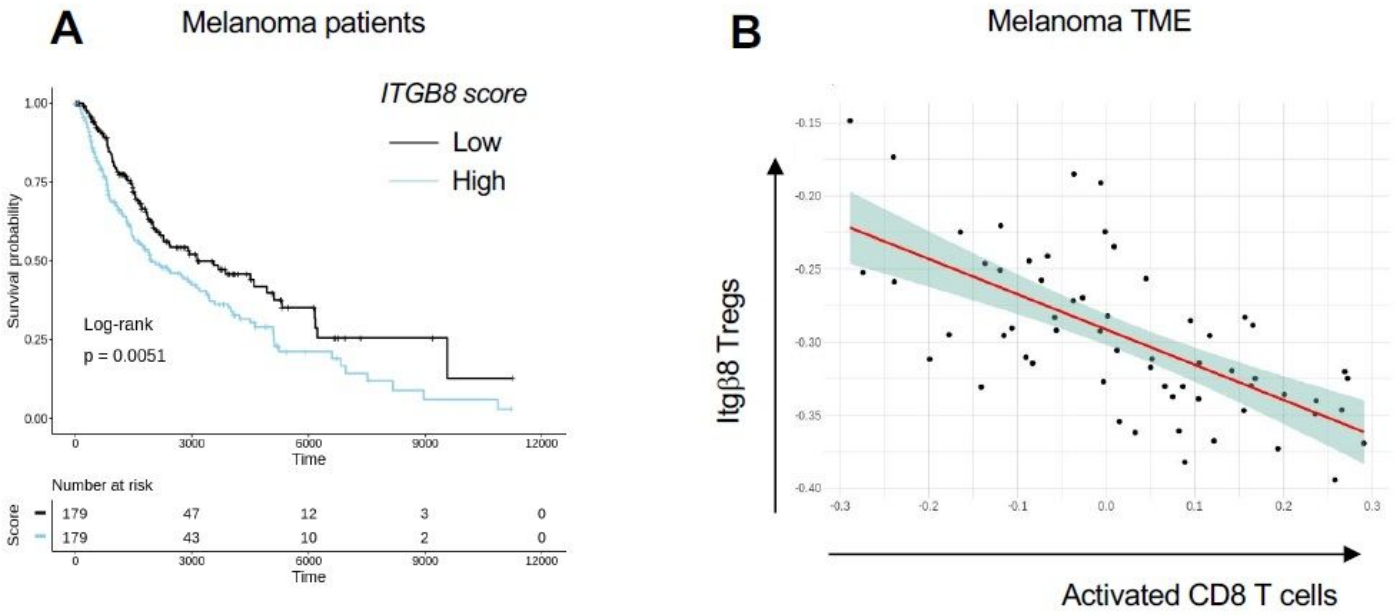

Figure 6

High Itgb8 score on T cell infiltrating melanoma correlates with patient worse prognostic and CD8 T cell activation in the TME. Transcriptome signatures of Itgb8pos Treg cells from patient melanoma were extracted from single cell RNAseq data (as described in Methods). The extracted signatures were used for testing their association with overall survival on The Cancer Genome Atlas (TCGA) RNAseq data from melanoma. Tumor samples were classified into low and high, based on the expression on ITGB8 score. A) Graph illustrates the overall survival of cancer patients stratified by ITGβ8 score in tumor infiltrating T cells with time expressed in days. n = 358 patients, 179 patients with high expression, 179 patients with low expression log rank p = 0.0051 using Mantel Cox test. B) Graph illustrating the inverse correlation between with ITGb8 Tregs core and activated CD8 T cell score in the same melanoma. Each dot represent one tumor. Spearman R value of correlation: -0.67

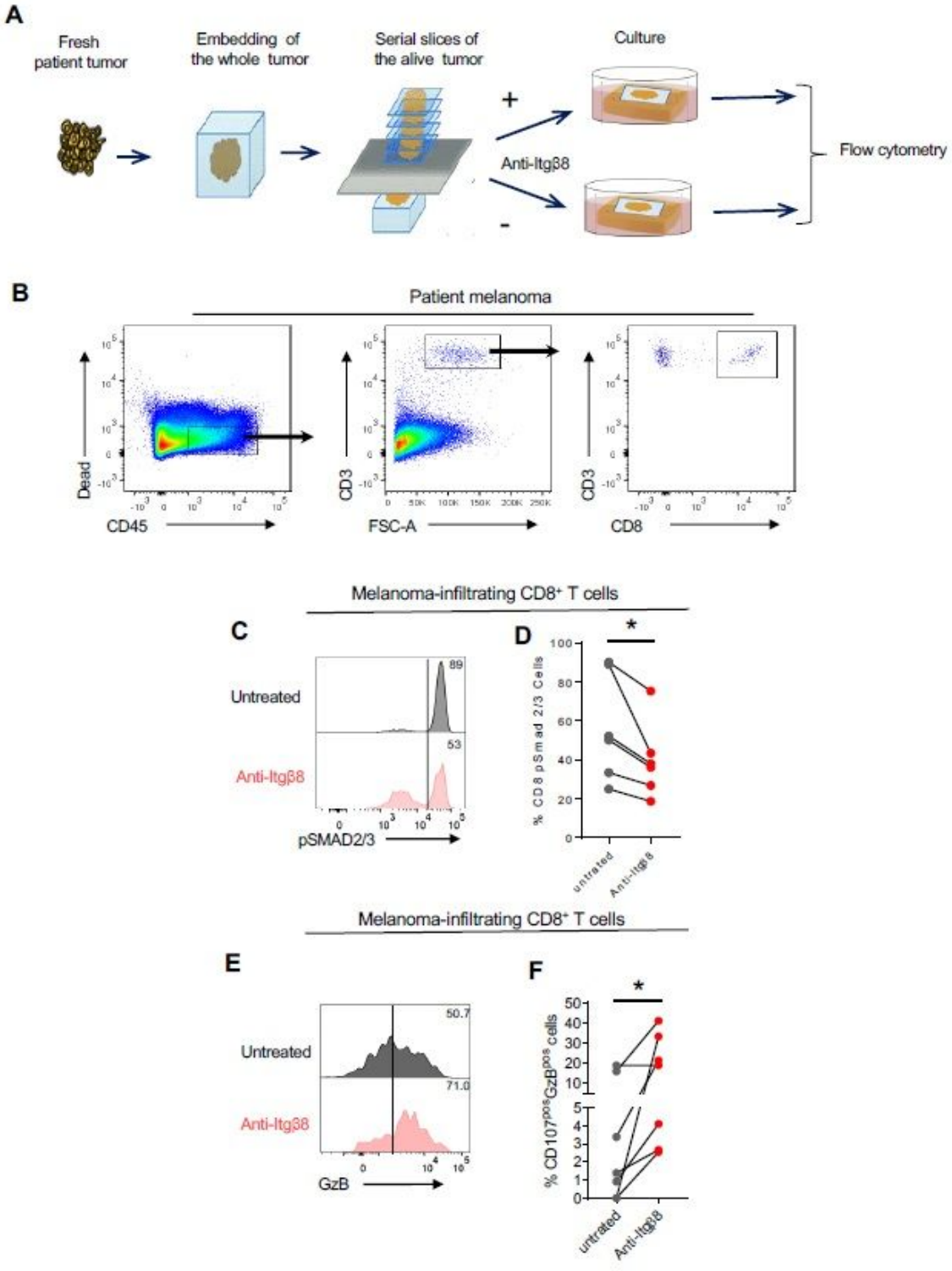

Figure 7

Targeting Itgβ8 in melanoma patients impairs TGF-b signaling and increases cytotoxic functions in tumor infiltrating CD8pos T cells. Fresh serial sections from a same melanoma for each patient were maintained in culture conditions in the presence or not of neutralizing anti-Itgb8 antibody as illustrated in A. B-E 48 hours later CD8pos T cells infiltrating the tumors were analyzed by flow cytometry as illustrated in B. C Representative histograms of the levels of phosphorylated SMAD2/3 (pSMAD2/3) in tumor

CD8pos T cells in the response to anti-Itgb8 antibody treatment. Percentages of cells with high levels of phosphorylation of SMAD2/3 are indicated. D Graph illustrates the percentage of CD8pos T cells positive for pSMAD2/3 in response to treatment. Each grey dot illustrates the value for tumor CD8pos T cells in the absence of treatment and the linked red dot that of CD8 T cells from the same tumor after anti-Itgb8 antibody treatment. E Representative histograms of the levels of granzyme B (GzB) in tumor CD8pos T cells in the response to anti-Itgb8 antibody treatment. Percentages of cells producing high levels of GzB are indicated. F Graph illustrates the percentage of CD8pos T cells positive for both GzB and CD107 in response to treatment. Each grey dot illustrates the value for tumor infiltrating CD8pos T cells in the absence of treatment and the linked red dot that of CD8pos T cells from the same tumor after anti-Itgb8 treatment. n=6-7 different patients, *p < 0.05 was determined by Wilcoxon test.

Supplementary Files

This is a list of supplementary files associated with this preprint. Click to download.

- FigureS1.jpg
- FigureS2.jpg
- FigureS3.jpg
- FigureS4.jpg
- FigureS5.jpg
- FigureS6.jpg